Steady-Flow Characteristics and Its Influence on Spray for Direct Injection Diesel Engine

Seung-hwan Choi, Chung-hwan Jeon*, Young-june Chang
School of Mechanical Engineering, Pusan National University San30, ChangJun-Dong, KumJeong-Ku, Pusan 609-735, Korea

Flow and spray characteristics are critical factors that affect the performance and exhaust emissions of a direct injection diesel engine. It is well known that the swirl control system is one of the useful ways to improve the fuel consumption and emission reduction rate in a diesel engine. However, until now there have only been a few studies on the effect of flow on spray. Because of this, the relationship between the flow pattern in the cylinder and its influence on the behavior of the spray is in need of investigation. First, in-cylinder flow distributions for 4-valve cylinder head of DI (Direct Injection) Diesel engine were investigated under steady-state conditions for different SCV (Swirl Control Valve) opening angles using a steady flow rig and 2-D LDV (Laser Doppler Velocimetry). It was found that swirl flow was more dominant than that of tumble in the experimented engine. In addition, the in-cylinder flow was quantified in terms of swirl/tumble ratio and mean flow coefficient. As the SCV opening angle was increased, high swirl ratios more than 3.0 were obtained in the case of SCV -70° and 90°. Second, spray characteristics of the intermittent injection were investigated by a PDA (Phase Doppler Anemometer) system. A Time Dividing Method (TDM) was used to analyze the microscopic spray characteristics. It was found that the atomization characteristics such as velocity and SMD (Sauter Mean Diameter) of the spray were affected by the in-cylinder swirl ratio. As a result, it was concluded that the swirl ratio improves atomization characteristics uniformly.

Key Words: DI (Direct Injection) Diesel Engine, SCV (Swirl Control Valve), LDV (Laser Doppler Velocimetry), PDA (Phase Doppler Anemometer), TDM (Time Dividing Method)

1. Introduction

The government has been imposing stricter diesel fuel efficiency standards to reduce carbon dioxide, NOx and other particulate emissions. Owing to the regulation on CO_2 emissions-for example the climate change convention-an engine needs to be developed that improves the reduction rate of the exhaust emission and specific fuel consumption simultaneously. Many of the technically advanced countries and automobile makers have been considering small DI (direct injection) diesel engines as one of the most suitable technologies (Hikosaka, 1997; Pischinger, 1998). One of the key technologies in DI diesel engines is to match fuel injection with proper in-cylinder swirl level, which is still being developed through much research (Ogawa et al., 1996). For an injector with several nozzle holes, relatively low swirl levels are sufficient to mix the fuel spray efficiently with the air. This is an advantage of the DI diesel engine over IDI (in-direct injection) diesel engines that need a high swirl level. To improve the reduction rate of the specific fuel consumption and emissions by controlling the swirl generation level

* Corresponding Author,
E-mail : chjeon@pusan.ac.kr
TEL : +82-51-510-3051; **FAX** : +82-51-512-9835
School of Mechanical Engineering, Pusan National University San30, ChangJun-Dong, KumJeong-Ku, Pusan 609-735, Korea. (Manuscript **Received** September 4, 2001; **Revised** April 17, 2002)

using an SCV (swirl control valve), it is of much interest to understand the flow pattern in the cylinder and its influence on the behavior of the spray.

The purpose of this study is to find out the relationship between the spray and flow patterns, and the effect of flow on the behavior of the spray. First, a steady-state rig test is conducted with an SCV (Lee et al., 1993; Furuno et al., 1990) to find parameters such as swirl ratio and the flow pattern in the cylinder (Snauwaert et al., 1986; Urushihara et al., 1995). On this basis, swirl flow field is visualized by 2D-LDV, and then the spray characteristics are analyzed using the PDA method (Quoc et al., 1994; Ishima et al., 1997; Giorgio et al., 1995).

2. Experimental Procedure

2.1 Text engine and SCV's shape

The steady-state experiments were performed with a direct injection diesel engine and the engine specifications are listed in Table 1. The intake ports consisted of two different ports : the tangential port and the helical port. The swirl-type SCV was installed in the tangential port side to control swirl ratio by varying the flow rate. The geometry and definition of the SCV opening angles are shown in Fig. 1. The SCV was controlled by the step with the unit of 10°.

The wide-open condition of the SCV was defined as 0° and controlled by the incremental step of 10°, that is, SCV ±90° denotes the close of the tangential port with the SCV. The reference state represented as the "Base" was taken without the SCV to compare with the SCV 0°. This experiment was performed with different SCV angles. The intake valve lifts were changed up to 9mm by the increment of 1.5mm.

2.2 Steady-state flow experiment

The schematic diagram of the steady-state test rig and 2D-LDV experiments is illustrated in Fig. 2. Two compressors with a capacity of 520 l/min were used to induce the intake air, and the flow rate was measured by the laminar flow meter with a capacity of 160 CFM (ft^3/min).

Table 1 Engine specification

Type	Direct injection diesel
Cylinder arrangement and number	In-line, 4 cylinders
Combustion chamber	Re-ENTRANT
Valve system	4 valve DOHC
Displacement (cc)	2902
Bore×Stroke (mm)	97.1×98

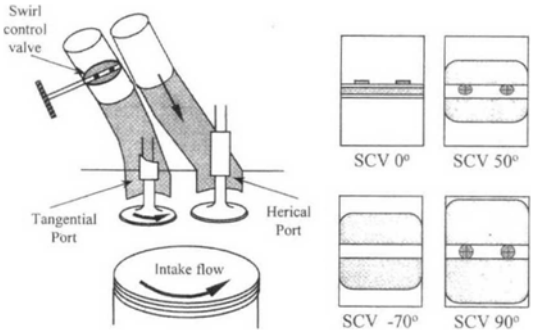

Fig. 1 Geometry and definition of SCV opening angle

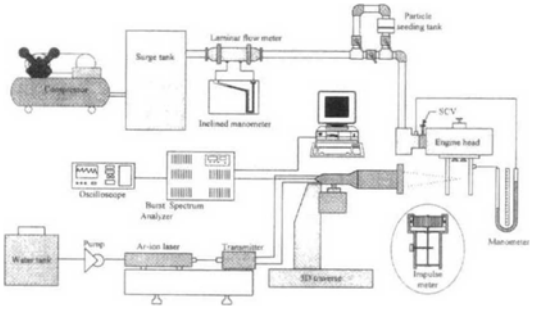

Fig. 2 Schematic diagram of steady-state test rig and 2D-LDV experiments

The intensity of swirling motion was converted to impulse torque using a swirl impulse meter, which was used to evaluate the flow coefficient (C_f), and non-rig swirl/tumble ratio ($NR_{s,t}$), mean flow coefficient ($\bar{C}_f$), and swirl/tumble ratio ($R_{s,t}$). The definitions of each parameter are as follows (Arcoumanis et al., 1989; Stone et al., 1992):

$$C_f=\frac{\dot{Q}}{AV_0} \tag{1}$$

$$NR_{s,t}=\frac{8\tau}{\dot{m}BV_0} \tag{2}$$

$$\bar{C}_f=\frac{\int_{\alpha_1}^{\alpha_2} C_f d\alpha}{\alpha_2-\alpha_1} \tag{3}$$

$$R_{s,t}=\frac{L_D\int_{\alpha_1}^{\alpha_2} C_f N R_{s,t} d\alpha}{\left\{\int_{\alpha_1}^{\alpha_2} C_f d\alpha\right\}^2} \tag{4}$$

$$L_D=\frac{BS}{N_v d_v^2} \tag{5}$$

where $\dot{Q}$ is the volume flow rate (m^3/s), A is the area of the intake port (m^2), V_0 is the maximum velocity through the intake port (m/s), τ is an impulse meter torque (N·m), $\dot{m}$ is a mass flow rate (kg/s), B is bore diameter (m), S is the stroke (m), α_1 is the intake valve open angle (radian), α_2 is the intake valve close angle (radian), N_v is the number of valves, d_v is the minimum valve diameter (m), and L_D is a shape factor including bore diameter, stroke, number of valves and minimum valve diameter.

Table 2 Specification of LDV system

Items	Units	Green beam	Blue beam
Wave length	nm	514.5	488.0
Focal length	mm	310.0	310.0
Beam separation	mm	72.0	72.0
Half angle of intersecting beams	deg.	6.78	6.78
Fringe spacing	μm	2.23	2.12
Number of fringe		35	35
Probe volume dimensions	Delta x [mm]	0.171	0.162
	Delta y [mm]	0.170	0.161
	Delta z [mm]	0.470	0.394

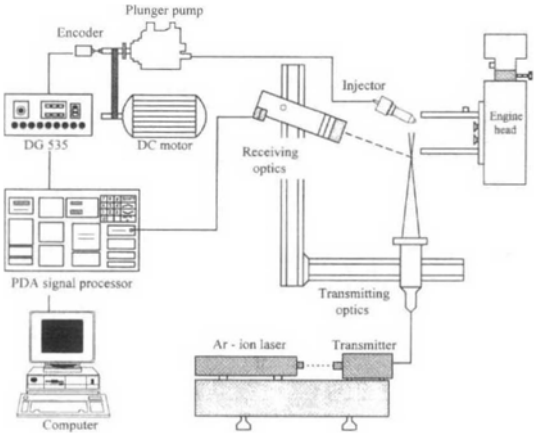

Fig. 3 Schematic diagram of PDA experiment

The 2D-LDV system was composed of a 5W Ar-ion laser, fiber optics, 3D traverse, signal processors and a data acquisition system. An LDV measurement based on the burst spectrum analyzer as signal processor was accomplished by backward scattering mode where focal length of the focal lens was 310mm. Al_2O_3 particles of 1 μm were seeded into the cylinder. The data acquisition system consisted of a BSA (Burst Spectrum Analyzer) and an IBM PC 586 through a GPIB interface. The specification of the LDV system is shown in Table 2.

Experiments for the effect of swirl flow interaction on spray characteristics were performed with the PDA system shown in Fig. 3. The cylinder head was rotated by 90(to see the effect of flow on the spray, and the fuel was injected into the cylinder. The fuel supplying pump, whose speed was detected by the encoder, was operated simultaneously with the PDA processor. The specification of the PDA system is shown in Table 3 and Table 4.

Only a single spray among the 6-hole VCO (Valve Closed Orifice) nozzle was measured by the PDA system. This nozzle was operated with two springs. The first opening pressure was 218 bar and the second opening pressure 324 bar. Figure 4 shows the behavior of pressure and needle lift with time. In this case, the revolution

Table 3 Specification of transmitting optics

Items	Units	Value
Fringe spacing	μm	4.4378
Number of fringes		34
Delta x	mm	0.1506
Delta y	mm	0.1504
Delta z	mm	2.5950
Wave length	nm	514.5
Gaussian beam diameter	mm	1.35
Beam collimator exp.		1
Beam expander exp.		1
Beam separation	mm	36
Lens focal length	mm	310

Table 4 Specification of receiving optics

Items	Units	Value
Maximum diameter	μm	80.773
Angle adjustment	mm	1.0
Scattering angle	deg.	45
Lens focal length	mm	310
Polarization angle	deg.	0
Direction of fringe motion		Positive
Particle/medium refraction indexes		1.46
Polarization orientation	(transmitter)	Parallel
Fringe rotation angle.	deg.	0
Optical frequency shift.	MHz	40
Doppler frequency bandwidth	MHz	36

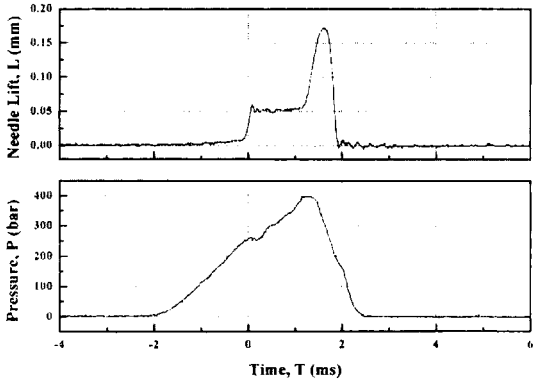

Fig. 4 Variation of pressure and needle lift with the time at 400 rpm

of the plunger pump was 400 rpm, therefore the revolution of the engine was 800 rpm. The injection duration was about 2 ms, maximum pressure was 400 bar and the maximum needle lift was 0.17 mm.

To improve the experimental accuracy of the 6-hole VCO nozzle, the experiment had to be carried out using only one hole. Unfortunately, there were interactions with the droplets injected from the 6 holes. This brought about several problems such as the decrease of experimental accuracy and validation plus lens contamination problems. So in this study, the VCO nozzle cap was modified to investigate only a single hole among the 6 holes. The nozzle cap is shown in Fig. 5.

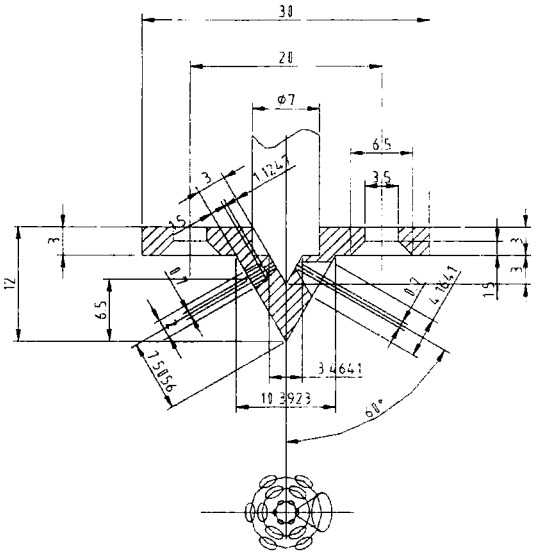

Fig. 5 Drawing the VCO nozzle cap

2.3 Emexperimental condition

Swirl strength was acquired by the constant differential pressure method, and the swirl impulse meter was installed at the position of 1.75×bore diameter down the cylinder head (Arcoumanis et al., 1989). Tumble intensity was obtained using a L-type induction tube to transform the tumble flow into swirl flow. The tumble measurement location was determined at the position of 3×bore diameter. To determine the measurement locations, the particles' trajectory, which was obtained to reveal overall behavior of swirl flow, was acquired as shown in Fig. 6. Analysis of the swirl using the 2-D LDV was accomplished at the two planes, which were selected to be 40 mm and 100 mm away from the cylinder head, based on the particles' trajectory. The SCV opening angles were selected as 0°, 50°, -70° and 90° from the result of the steady-state rig test. Swirl flow was measured at 57 points, every 10 mm distance from the center of the section. The PDA experiment was conducted under flow and non-flow conditions in terms of SCV opening angles and the number of measurement data was 12,000 at every point. According to Lefebvre (1989), to achieve a reasonably accurate estimate of spray quality, it is necessary to measure about 5,500 drops, as this results in

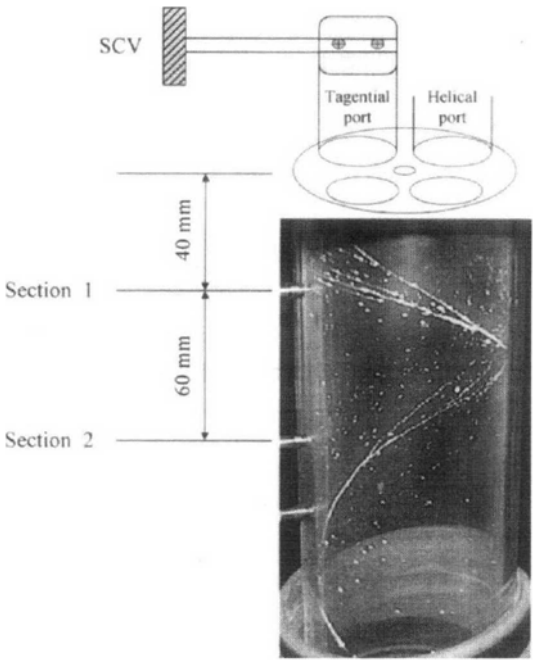

Fig. 6 Path-line of particles for swirl flow and measurement sections

a 95% confidence limit. So it can be concluded that the accuracy of the PDA experiments is over 95%.

3. Results and Discussion

3.1 Steady-state flow

Figure 7 shows a correlation between the mean flow coefficients and the swirl ratios. In the "Base" case, the value of the mean flow coefficient is 3% larger than that of the SCV 0° case. As the SCV opening angle increases, the value of the swirl ratio becomes larger and is contained within a range of 2.3~3.8. According to the results of Made et. al., (1998) the range of the swirl ratio for maintaining a stable engine performance is 3~4 in a high rpm region. In this experiment, the swirl ratios that satisfied these criteria are above the SCV 60°. The mean flow coefficient is found to be in an inverse proportional relationship to the swirl ratio. This means that as the opening ratio of the SCV is decreased, the swirl generation capability is increased. From this result, the swirl ratio is confirmed in an trade-off relation to the mean flow coefficient.

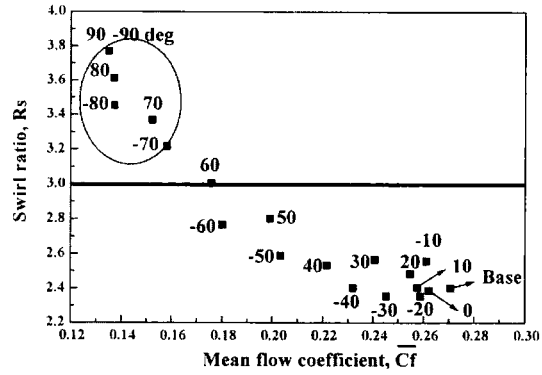

Fig. 7 Correlation between mean flow coefficient and swirl ratio

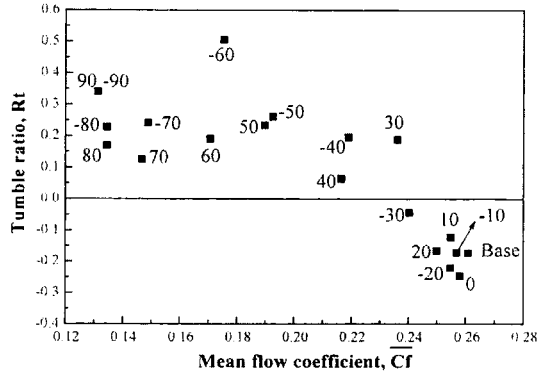

Fig. 8 Correlation between mean flow coefficient and tumble ratio

Figure 8 shows the correlation between the mean flow coefficient and the tumble ratio. The mean flow coefficient has the largest value in the base case, and also has almost the same values as the SCV angle signs. The tumble ratio is much lower than that of the swirl ratio by about 10% since the SCV installed on the tangential port is focused on intensifying the swirl flow in two different ports system. Due to this result, further studies should be conducted on swirl flow.

3.2 Flow characteristics

Analysis of the swirl flow using 2D-LDV was conducted at the two planes. The selected cross-sections were the planes 40 mm and 100 mm away from the cylinder head as shown in Fig. 6. Figure 9 illustrates the velocity distribution of

the cross-sectional flow field in the cases of SCV 0° (swirl ratio 2.4), SCV 50° (2.8), SCV -70° (3.2) and SCV 90° (3.8). The first two graphs in the case of SCV 0° represent the results of raw velocity data measured by 2D-LDV. The others are the results of interpolation of the two velocity data by the inverse distance method. Figure 9(d) and 9(e) are the results of SCV -70° and SCV 90° with the swirl ratio over 3.0, respectively. In cross-section 1, which is 40 mm apart from the top of the cylinder head, the swirl motion is weakly developed in a comparably early stage, but it is fully developed in cross-section 2 100 mm farther down. Especially in cross-section 2 with SCV 90°, the center of swirl is located in the near center of the cylinder. In the cases of SCV 0° and SCV 50°, the swirl flow is formed early at section 1, but it does not develop any further. In these cases, the swirl ratios are lower than those of other cases but the flow coefficients are relatively high. For this reason, velocity magnitudes are illustrated largely in the measurement point.

Due to the rigid body rotation induced by the higher swirl flow, its axis slightly moves from near the intake ports to the central axis of the cylinder down stream, which seems to become the source of turbulence at the end of the compression (Kang et al., 1999).

To quantify the mean velocity of each section, the values of each velocity are averaged for SCV opening angles as shown in Fig. 10. Before the calculation was performed, it was thought that the mean velocity of section 1 would have a larger value than that of section 2. But it was found that the mean velocity of section 1 has a lower value than that of section 2 in all cases. Actually, the flow is rapidly induced through the intake ports and then enters the cylinder in the form of swirl or tumble depending on the configuration of the intake ports and the existence of SCV. When the flow passes through the upper section, it does not yet swirl. However, as the flow goes downstream, it seems to perform stronger swirls than that of the upper section. In addition, the result is in good accordance with the magnitude of the velocity vector shown in Fig. 9. As the SCV opening ratio is increased, it is observed that the mean velocity becomes smaller without regard to the cross-sections. This result is well consistent with the relationship between the swirl ratio and the mean flow coefficient as mentioned in Fig. 7.

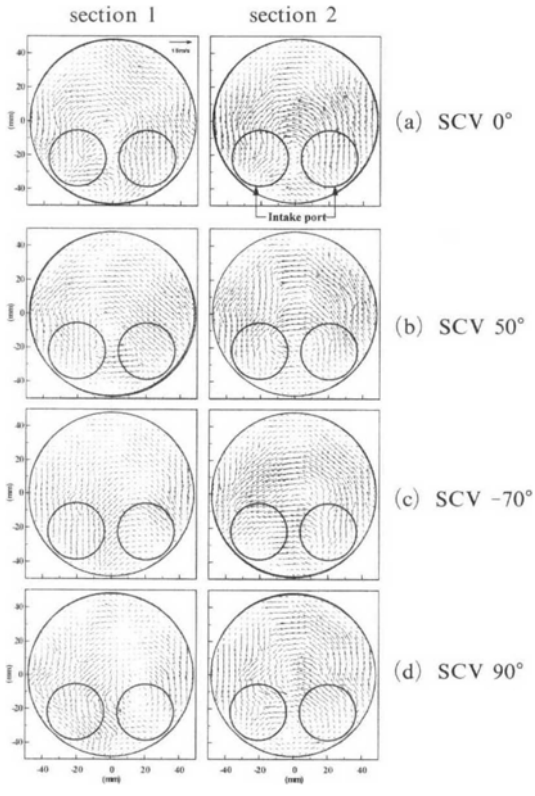

Fig. 9 Swirl flow patterns for different SCV opening angles

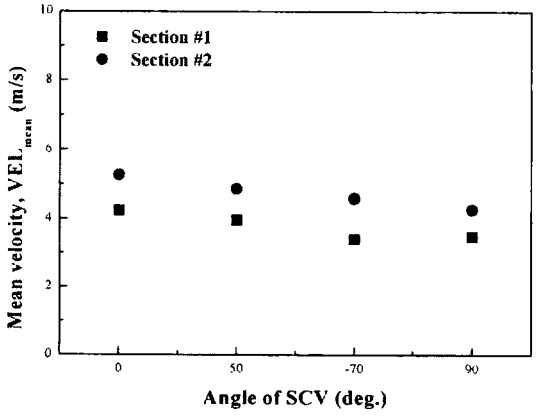

Fig. 10 Mean velocity with SCV opening angles

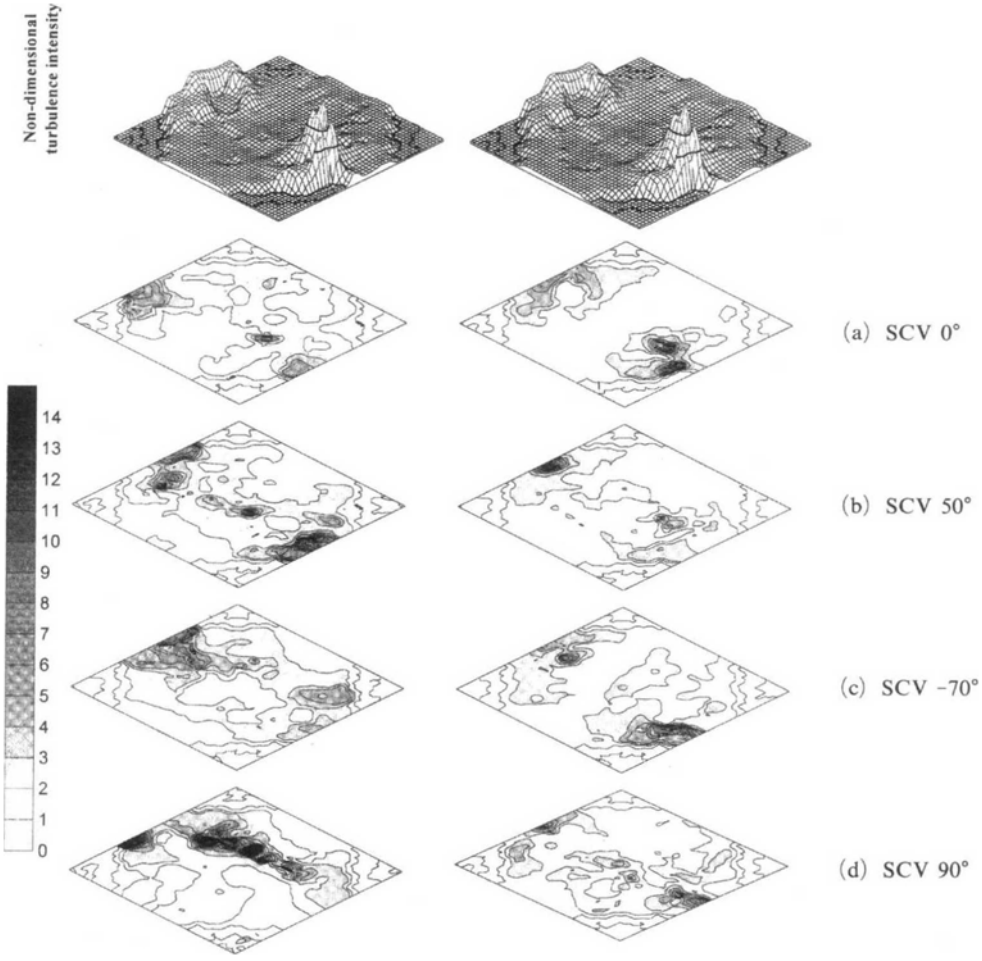

Fig. 11 Distribution of non-dimensional turbulence intensity

Figure 11 shows the contour of turbulence intensity, which is the ratio of r.m.s. of velocity to each velocity at 1,024 interpolated points. In the figure, the label of 'X pixel' denotes the intake valve side as shown in Fig. 12. In all cases except SCV 90° at cross-section 1, the locations that have high turbulence intensity only exist in the downward region of the intake valve and/or exhaust valve. Furthermore the region of turbulence intensity level over 1 is more widely dispersed in section 1 than that in the section 2. This means that cross-section 2 has a more stable swirl structure compared to section 1.

It is important to know the velocity distribution in the flow field, so non-dimensional velocity is defined as

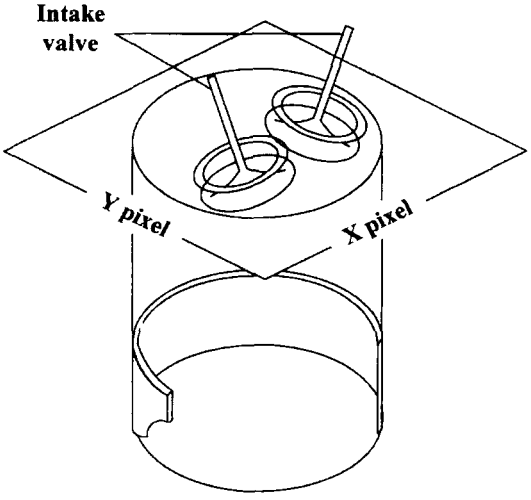

Fig. 12 Schematic diagram of concerned region

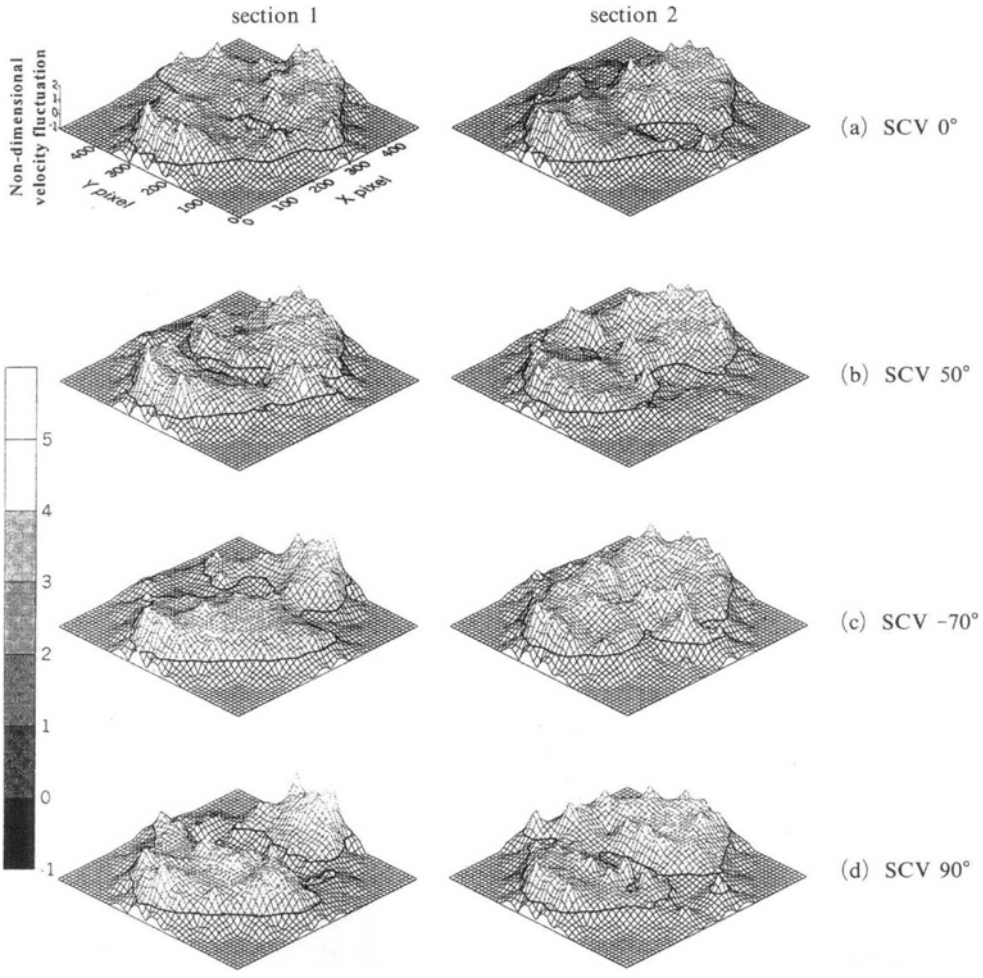

Fig. 13 Distribution of non-dimensional velocity fluctuation

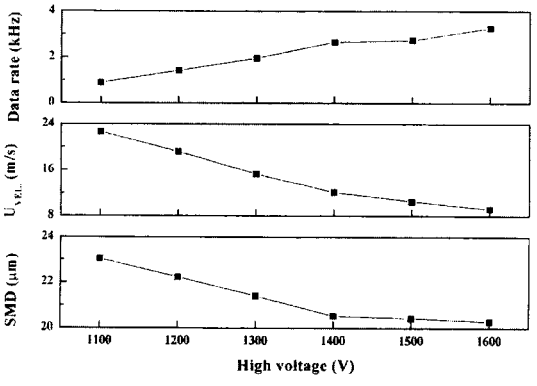

Fig. 14 Effect of different high voltage on data rate, average velocity and SMD

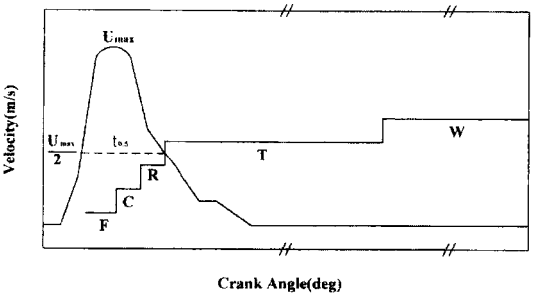

Fig. 15 Concept diagram of Time dividing method

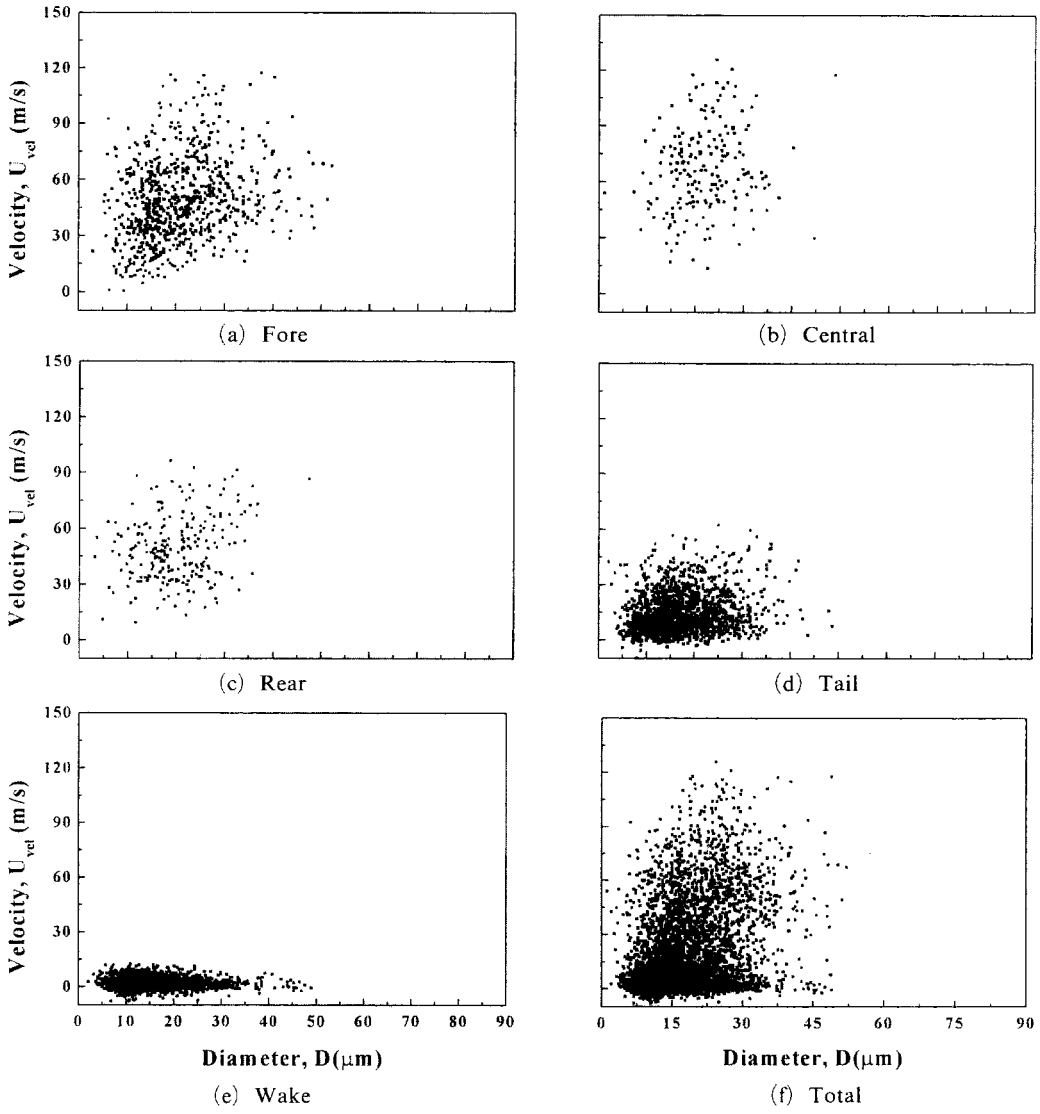

Fig. 16 Temporal spray characteristic with non-flow condition at 400 rpm

$$N.V.=\frac{V-V_{mean}}{V_{mean}} \tag{6}$$

Figure 13 shows the distribution of non-dimensional velocity for each condition. When the value of non-dimensional velocity is larger than 0, this means the local velocity has a higher value than that of mean velocity. So the value of 0 means that the local velocity and the mean velocity have the same value. The solid contour line indicates that the non-dimensional velocity is zero. In cross-section 1, high non-dimensional velocity is concentrated in special regions, especially the wall region. But in cross-section 2, the values are wide compared to section 1 although the values are somewhat lower. From this result it is confirmed that a more stable swirl structure is observed in section 2 compared to the upper section once again.

3.3 Spary characteristics

In the PDA experiment, the high voltage power supply for each PMT (photo-multiplier tube) is a very important factor. The high voltage can be set

from 0 to 20,000V in 8V increments. Generally, when the voltage is reduced, the transit time in the PMT will increase and thus cause phase errors resulting in incorrect measurements of the size; spherical particles may be rejected as being non-spherical. So, as the high voltage is increased, the result of the SMD (Sauter mean diameter) is smaller than that of its actual size.

To decide on optimal high voltage, the effects of high voltage on the characteristics of spray from 1,100 to 1,600V in 100V increments was investigated. The measurement location is 30mm downstream from the nozzle tip. Figure 14 shows the effect of high voltage on the data rate, average velocity and SMD. In the case of data rate, as high voltage is increased, it increases from 1,100 to 1,400V, and after 1,400V it changes very little. In the case of average velocity and SMD, it decreases rapidly until 1,400V and then decreases slowly. As mentioned above, it is confirmed that the high voltage has an inverse proportional relationship to the SMD. In addition, above 1,400V, the average velocity and SMD are not affected by the value of high voltage. So in this experiment, high voltage was determined to be about 1,400V.

First, the experiment is carried out under non-flow conditions in which it has meaning as the reference value for the flow condition experiment. The time dividing method (T.D.M.) is applied to evaluate the intermittent spray as shown in Fig. 15. This method is needed to define the phase duration t0.5 where the velocity of droplets is larger than the half value of the maximum. The t0.5 is divided equally into 3 parts where each part is represented by the fore (F), central (C) and rear (R) parts, in turn. The central part includes the largest velocity of droplets. After that, the tail (T) part with three times the duration of the t0.5 is determined, and the rest of the time is the wake (W) part. Dividing the intervals of intermittent spray like F, C, R, T, and W has the advantage of getting information about velocity and droplet size at the narrower crank angle interval.

Figure 16 shows the correlation between velocity and droplet size at 130 mm down stream of the nozzle at 400 rpm of the injection pump in the case of non-flow conditions. Figure 16(a) is the fore part in which velocity and droplet diameter have widely distributed values compared to Figs. 16(b) ~ (e). It could be considered as an early stage of injection. Figure 16(b) is the central part in which velocity has a large value but droplet diameter is somewhat small because it could be regarded as the mid-stage of injection at the most vigorous time. The velocity is inclined to decrease slightly in the rear part (c) which is the end stage of injection. Figure 16(d) is the tail part just after injection is finished. The velocity becomes quite lower than before and characteristics of atomization get better. Figure 16(e) is the wake part which has droplets with a velocity close to zero and a broad distribution of large droplet diameters. Figure 16(f) sums up all temporal parts.

The influences of swirl flow on atomization are covered with the flow condition at SCV angle 0°, 50°, -70° and 90°. Figure 17 is the result that is analyzed by TDM with SCV 90° at 400rpm. Figure 17(f) is the total result. There is no difference to Fig. 16(f). But the result of each part gives different aspects to non-flow conditions. In the fore part (a), droplets have lower velocity contrary to the non-flow. That is the reason why the swirl flow has an effect on the injected droplets : the droplets lose their own momentum as they interact with the swirl flow. The central (b) and rear(c) parts have a similar tendency, but the droplets with flow in (d) and (e) have a wide range of velocities, which contain low velocities and large droplets.

The mean velocity change of with/without flow through the whole injection time is shown in Fig. 18. During the injection timing, droplets under non-flow conditions have large velocity values, especially the central part which has the highest velocity. After the injections, they have very low velocities because pressure momentum was not provided against air drag. The mean value of velocity with flow conditions shows totally different patterns against non-flow conditions. The values are within some ranges along the whole of the parts. Also the velocity along the temporal part was moderated by the swirl flow.

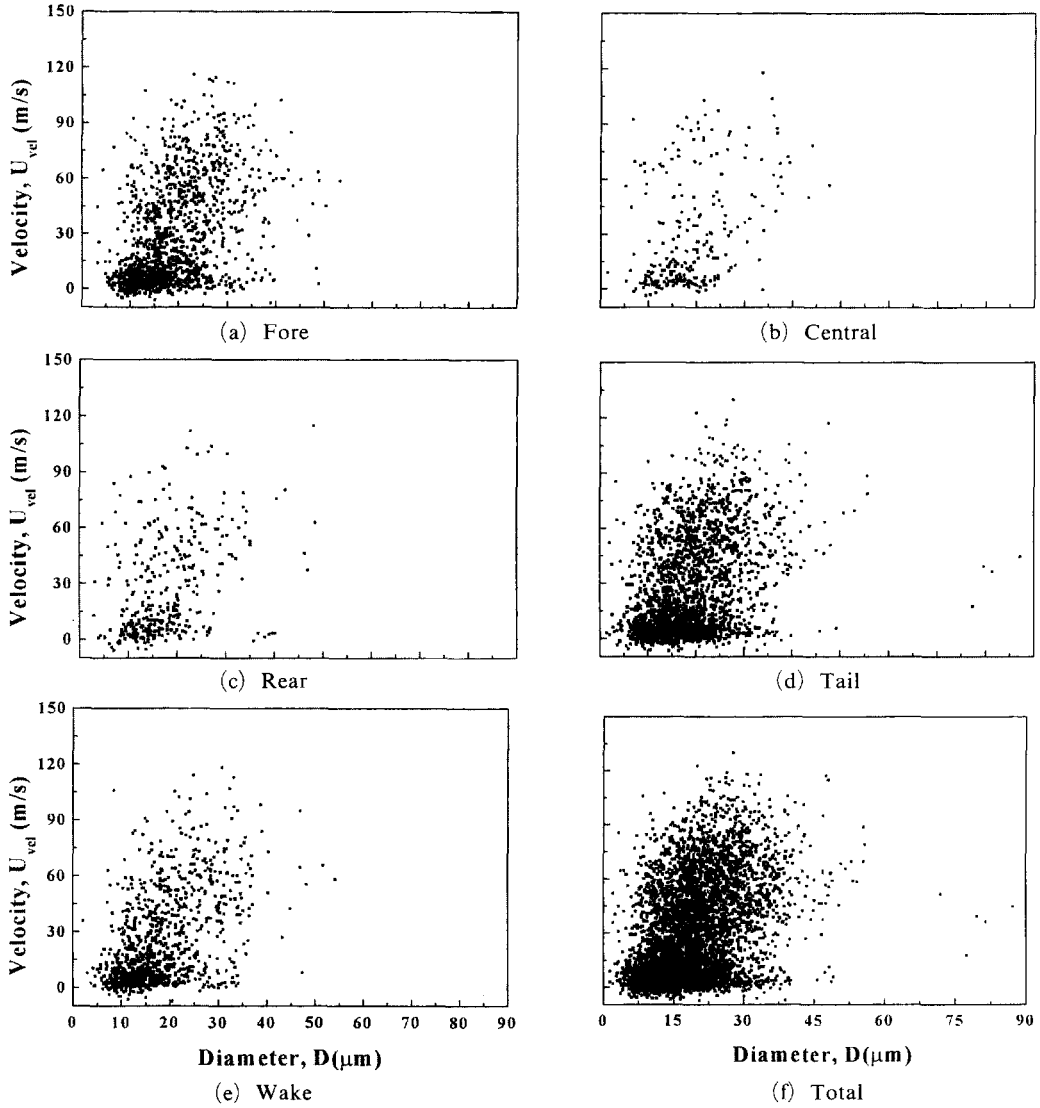

Fig. 17 Temporal spray characteristic with SCV 90° condition at 400rpm

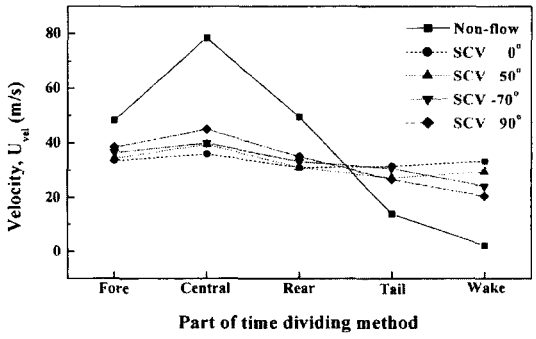

Fig. 18 Effect of swirl flow on temporal velocity characteristic

Figure 19 shows the SMD of each temporal part in the intermittent spray. Generally, without flow, the droplets have a broad SMD distribution by the collision mechanism which displays high velocity momentum characteristics in the early stage of injection. When the injection is finished, the SMD becomes a small value by the effects of the ambient gas entrainment. Contrary to no-flow cases, the SMD difference under flow conditions existed within a 1~2 μm range regardless of the temporal part in each SCV angle. In addition, the velocity and SMD differences along the temporal

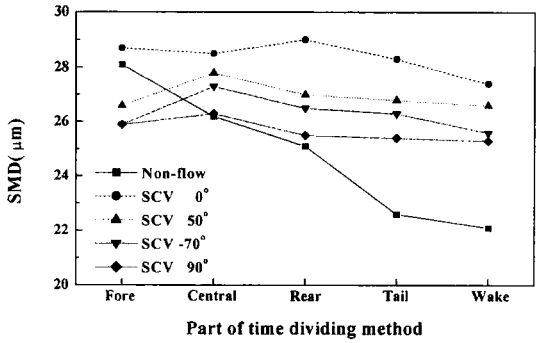

Fig. 19 Effect of swirl flow on temporal SMD characteristic

part were moderated by the swirl flow. From these results, it is concluded that the swirl ratio improves atomization uniformly.

4. Conclusion

The steady-flow characteristics of a DI diesel engine were analyzed through changes of opening angles of a SCV mounted on two independent intake ports. On this basis, the experiments utilizing 2D-LDV for flow and PDA measurement for spray were performed to derive the following:

(1) As an SCV opening angle increases in the tangential port, the swirl ratio decreases and it is contained within a range from 2.3 to 3.8 in a steady-state rig test. High swirl ratios more than 3.0 can be obtained in the case of SCV -70° and 90°. But the tumble ratio is contained within a very small range such as $-0.3 \sim 0.5$.

(2) Based on the results of the swirl ratio, 2D visualization was conducted for 4 different SCV angles by using a 2D-LDV system. In the case of high swirl conditions over 3.0 (SCV -70° and 90°), the swirl motion is not readily found in cross-section 1, but it is fully developed in cross-section 2. Especially in the case of SCV 90°, the center of swirl is located in the near center of the cylinder in cross-section 2, and it seems to become the source of turbulence at the end of compression

(3) In the PDA experiment, it was found that high voltage is a very important factor and an optimal value was determined to be 1,400 V. The spray characteristics were analyzed by using a time dividing method. The total relationship between droplet diameter and velocity is not different between cases of with and without flow conditions. However the result of each part gives different aspects. The velocity and SMD difference along the temporal part are moderated by the swirl flow, and the swirl ratio improves the atomization characteristics uniformly.

References

Arcoumanis, C. and Tanabe, S., 1989, "Swirl Generation by Helical Ports," SAE Paper 890790.

Furuno, S. and Iguchi, S., 1990, "The Effects of 'Inclination Angle of Swirl Axis' on Turbulence Characteristics in a 4-Valve Lean-Burn Engine with SCV," SAE Paper 902139.

Giorgio, F. D. and Laforgia, D., 1995, "Investigation of Drop Size Distribution in the Spray of a Five-Hole, VCO Nozzle at High Feeding Pressure," SAE Paper 950087.

Hikosaka, N., 1997, "A View of the Future of Automotive Diesel Engines," SAE Paper 972682.

Ishima, T., Obokata, T., 1997, "Time Dividing Analysis of Intermittent Fuel Spray Flows Measured by PDA," ICLASS-97, Seoul.

Kang, K. and Reitz, R., 1999, "The Effect of Intake Valve Alignment on Swirl Generation in a DI Diesel Engine," *Experiment Thermal and Fluid Science*, pp. 94~103.

Lee, K. and Urushihara, T., 1993, "Analysis of Gas Flow Fields Generated by Butterfly type Swirl Control Valve," JSAE Paper 9304365.

Lefebvre. H., 1989, "Atomization and Sprays," Hemisphere Publishing Corporation.

Mase, Y., Kawashima, J. and Sato, T., 1998, "Nissan's New Multi-Valve DI Diesel Engine Series," SAE Paper 981039.

Ogawa, H., Matsui, Y. and Kimura, S., 1996, "3-D Computation of the Effects of the Swirl Ration in DI Diesel Engine on NOx and Soot Emissions," SAE Paper 961125.

Pischinger, F. F., 1998, "The Diesel Engine for Cars-Is There a Future," *J. Eng. For Gas Turbines and Power, Trans. ASME* 120, pp. 641~

647.

Quoc, H. X. and Brun, M., 1994, "Study on Atomization and Fuel Drop Size Distribution in Direct Injection Diesel Spray," SAE Paper 940191.

Snauwaert, P. and Sievens, R., 1986, "Experimental Study of the Swirl Motion in DI Diesel Engine Under Steady State Flow Conditions," SAE Paper 860026.

Stone, C. R. and Ladommatos, N., 1992, "The Measurement and Analysis of Swirl Steady-Flow," SAE Paper 921642.

Urushihara, T., Murayama, T. and Lee, K., 1995, "Turbulence and Cycle-by-Cycle Variation of Mean Velocity Generated by Swirl and Tumble Flow and Their Effects on Combustion," SAE Paper 950813.